

AD-A175 431

EXPLORATION OF THE POTENTIAL PERFORMANCE OF DIODE  
LASER-PUMPED GAS CELL A. (U) AEROSPACE CORP EL SEGUNDO  
CA CHEMISTRY AND PHYSICS LAB J C CAMPARO ET AL.

1/1

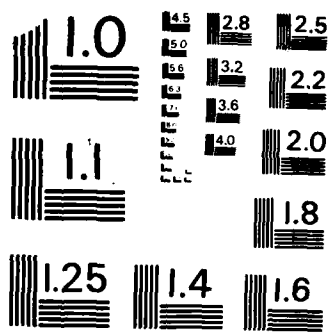
UNCLASSIFIED

30 SEP 86 TR-0006(6945)-2 SD-TR-86-64

F/G 14/2

ML





MICROCOPY RESOLUTION TEST CHART  
NATIONAL BUREAU OF STANDARDS - 1963 - A

12

AD-A175 431

# Exploration of the Potential Performance of Diode Laser-Pumped Gas Cell Atomic Frequency Standards

Prepared by

J. C. CAMPARO and R. P. FRUEHOLZ  
Chemistry and Physics Laboratory  
Laboratory Operations  
The Aerospace Corporation  
El Segundo, CA 90245

30 September 1986

APPROVED FOR PUBLIC RELEASE;  
DISTRIBUTION UNLIMITED

DTIC  
SELECTE  
DEC 30 1986  
S D

Prepared for

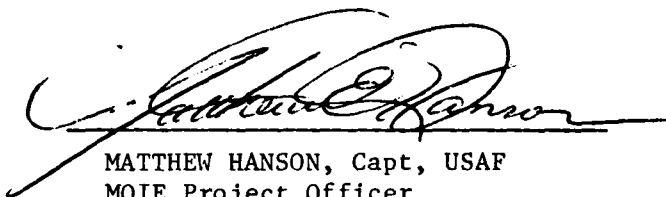
SPACE DIVISION  
AIR FORCE SYSTEMS COMMAND  
Los Angeles Air Force Station  
P.O. Box 92960, Worldway Postal Center  
Los Angeles, CA 90009-2960

DTIC FILE COPY

This report was submitted by The Aerospace Corporation, El Segundo, CA 90245, under Contract No. F04701-85-C-0086 with the Space Division, P.O. Box 92960, Worldway Postal Center, Los Angeles, CA 90009-2960. It was reviewed and approved by The Aerospace Corporation by S. Feuerstein, Director, Chemistry and Physics Laboratory. Captain Matthew Hanson, SD/YEZ, was the project officer for the Mission-Oriented Investigation and Experimentation (MOIE) Program.

This report has been reviewed by the Public Affairs Office (PAS) and is releasable to the National Technical Information Service (NTIS). At NTIS, it will be available to the general public, including foreign nationals.

This technical report has been reviewed and is approved for publication. Publication of this report does not constitute Air Force approval of the report's findings or conclusions. It is published only for the exchange and stimulation of ideas.



MATTHEW HANSON, Capt, USAF  
MOIE Project Officer  
SD/YEZ



JOSEPH HESS, GM-15  
Director, AFSTC West Coast Office  
AFSTC/WCO OL-AB

REPORT DOCUMENTATION PAGE		READ INSTRUCTIONS BEFORE COMPLETING FORM
1. REPORT NUMBER SD-TR-86-64	2. GOVT ACCESSION NO. ADA175431	3. RECIPIENT'S CATALOG NUMBER
4. TITLE (and Subtitle) EXPLORATION OF THE POTENTIAL PERFORMANCE OF DIODE LASER-PUMPED GAS CELL ATOMIC FREQUENCY STANDARDS		5. TYPE OF REPORT & PERIOD COVERED
7. AUTHOR(s) James C. Camparo and Robert P. Frueholz		6. PERFORMING ORG. REPORT NUMBER TR-0086(6945-05)-2
9. PERFORMING ORGANIZATION NAME AND ADDRESS The Aerospace Corporation El Segundo, Calif. 90245		8. CONTRACT OR GRANT NUMBER(s) F04701-85-C-0086
11. CONTROLLING OFFICE NAME AND ADDRESS Space Division Los Angeles Air Force Station Los Angeles, Calif. 90009-2960		10. PROGRAM ELEMENT, PROJECT, TASK AREA & WORK UNIT NUMBERS
14. MONITORING AGENCY NAME & ADDRESS (if different from Controlling Office)		12. REPORT DATE 30 September 1986
		13. NUMBER OF PAGES 23
		15. SECURITY CLASS. (of this report) Unclassified
		15a. DECLASSIFICATION/DOWNGRADING SCHEDULE
16. DISTRIBUTION STATEMENT (of this Report) Approved for public release; distribution unlimited.		
17. DISTRIBUTION STATEMENT (of the abstract entered in Block 20, if different from Report)		
18. SUPPLEMENTARY NOTES		
19. KEY WORDS (Continue on reverse side if necessary and identify by block number) Atomic Clocks Diode Lasers Optical Pumping,		
20. ABSTRACT (Continue on reverse side if necessary and identify by block number) Recently, there has been considerable interest in the use of single-mode diode lasers in atomic frequency standards. In this report, theoretical calculations were performed to quantify the expected performance improvement upon incorporation of diode lasers in rubidium gas cell atomic frequency standards. We assume that clock signal shot noise, the diode laser's quantum noise, and diode laser frequency locking noise all contribute to the atomic frequency standard's stability. Our results indicate that white		

UNCLASSIFIED

SECURITY CLASSIFICATION OF THIS PAGE(When Data Entered)

19. KEY WORDS (Continued)

20. ABSTRACT (Continued)

noise Allan variances of  $\sim 6 \times 10^{-15} / \sqrt{\tau}$  are possible if enhanced cavity Q diode lasers are employed, whereas for presently available commercial diode lasers we predict white noise Allan variances of  $\sim 3 \times 10^{-14} / \sqrt{\tau}$ . These variances represent 2 to 3 orders of magnitude improvement in frequency stability over that currently obtained with rubidium gas cell atomic clocks.

UNCLASSIFIED

SECURITY CLASSIFICATION OF THIS PAGE(When Data Entered)

CONTENTS

I. INTRODUCTION..... 5

II. OVERVIEW OF THE GAS CELL FREQUENCY STANDARD MODEL..... 7

III. LASER-PUMPED GAS CELL CLOCK..... 9

    A. Diffusion..... 9

    B. Laser Stability..... 11

    C. Atomic Standard Stability..... 14

IV. RESULTS..... 17

V. SUMMARY..... 23

REFERENCES..... 25



Accession For	
NTIS CRA&I	<input checked="" type="checkbox"/>
DTIC TAB	<input type="checkbox"/>
Unannounced	<input type="checkbox"/>
Justification .....	
By .....	
Distribution / .....	
Availability Codes	
Dist	Avail and/or Special
A-1	

## FIGURES

1.	Spatial Distribution of Hyperfine Polarization.....	10
2.	Full Width at Half Maximum of the Envelope Function Normalized to the Resonance Cell Length as a Function of the Relative Photon Absorption Rate.....	12
3.	Best Temperature and Rabi Frequency vs. Laser Power.....	18
4.	Allan Variance vs. Single-Mode Laser Intensity.....	19
5.	Comparison of Some Proposed Atomic Frequency Standards.....	24

## TABLES

1.	Parameters Used in the Calculation of the Clock Signal Shot Noise Contribution to the Diode Laser-Pumped Gas Cell Clock's White Noise Allan Variance.....	16
2.	Minimum Attainable Allan Variances of the Diode Laser-Pumped Rubidium Gas Cell Atomic Frequency Standard.....	20



## 1. INTRODUCTION

Recently, there has been considerable interest in and speculation on the use of single-mode diode lasers for optical pumping in atomic frequency standards. In particular, current efforts are primarily focused on the cesium beam frequency standard,<sup>1</sup> where atomic state preparation by diode laser optical pumping and atomic state detection by diode laser-induced fluorescence are envisaged as replacing the traditional A and B magnets of atomic beam standards. The impetus for this activity is the many possible advantages of optical state preparation and detection, for example greater signal-to-noise ratios,<sup>2</sup> and recent theoretical and experimental work would indicate that these expectations are well founded.<sup>3,4</sup> However, in addition to the cesium beam frequency standard work there has also been a growing interest in the area of diode laser optical pumping in rubidium gas cell frequency standards,<sup>5</sup> where it is anticipated that diode laser optical pumping will both improve the signal-to-noise ratio and drastically reduce light shift effects.<sup>6</sup> Unfortunately, in contrast to the cesium beam studies, to date, there have been no theoretical calculations to support these expectations or to provide insights into the choice of the optimal optical pumping conditions.

In order to remedy this situation the present series of theoretical calculations were undertaken. In particular, we consider a rubidium gas cell atomic frequency standard operating in its traditional configuration (i.e., cw optical pumping), except that the typical rf discharge lamp used for optical pumping is replaced by a single-mode diode laser tuned to the  $5^2P_{3/2}$  ( $F=0,1,2,3$ ) -  $5^2S_{1/2}$  ( $F=2$ ) optical absorption resonance of  $Rb^{87}$ . Furthermore, we assume that there is no filter cell, and that the resonance cell contains pure  $Rb^{87}$ . The calculations are performed in such a way that for a particular incident diode laser intensity we calculate the resonance cell temperature and peak microwave Rabi frequency that minimize the shot noise limited Allan variance as well as the minimum Allan variance itself. Additionally, we estimate the effect of frequency noise for a frequency stabilized diode laser on the frequency standard's performance. This noise is transferred to the

atomic standard via the light shift effect,<sup>7</sup> and as will be shown, it limits the ultimate frequency standard stability.

## II. OVERVIEW OF THE GAS CELL FREQUENCY STANDARD MODEL

In a previous publication we introduced and validated a nonempirical model of the gas cell atomic frequency standard.<sup>8</sup> Briefly, this model considers the relevant gas phase physics as occurring on two different scales. On the microscopic scale the 0-0 hyperfine transition lineshape of an arbitrary alkali atom of half-integer nuclear spin is determined by the generalized Vanier theory of alkali atom hyperfine optical pumping.<sup>9-10</sup> Among other parameters this theory considers the dependence of the hyperfine lineshape on optical pumping light intensity and microwave Rabi frequency. However, because the buffer gas pressure in a gas cell standard effectively freezes the alkali atoms in place on time scales of the order of a Rabi period,<sup>11</sup> and because the alkali vapor is not necessarily optically thin, these two parameters and, hence, the microscopic lineshape, vary from atom to atom within the vapor. Furthermore, as a result of diffusion to the resonance cell walls, where the atoms immediately depolarize on impact, there is a spatial distribution of hyperfine polarization  $\langle \hat{I} \cdot \hat{S} \rangle$ . In some sense this spatial distribution of  $\langle \hat{I} \cdot \hat{S} \rangle$  can be imagined as being superimposed on the microscopic physics. Thus, there is a macroscopic scale of physics in the problem which is related to both the spatial variation of optical pumping light intensity and microwave Rabi frequency, and the spatial distribution of  $\langle \hat{I} \cdot \hat{S} \rangle$  due to diffusion to the resonance cell walls.

To treat this macroscopic scale of physics in a reasonably lucid manner, the problem was reduced to one dimension, so that only the longitudinal variation of the optical pumping rate and microwave field strength was considered. This is reasonable because the microwave field can be made uniform in the transverse dimension by dielectrically loading the cavity, and because the laser intensity can easily be made uniform across the face of the resonance cell. The microwave Rabi frequency distribution along the axial dimension was determined by the microwave cavity mode, assuming that the atomic resonance cell filled the microwave cavity. The axial variation of the optical pumping light intensity was determined by computing a "global" optical

pumping parameter  $\zeta$  in a self-consistent manner. In essence, this global optical pumping parameter determined the fractional population in the optically absorbing hyperfine multiplet, and thus the optical depth of the vapor as a result of optical pumping. Since we assumed that the alkali atoms were effectively frozen in place in the resonance cell, the first order change in transmitted light intensity as a function of microwave Rabi frequency for a wedge of vapor of thickness  $dz$  only depended on the local values of the optical pumping light intensity and microwave Rabi frequency. To include the effect of axial diffusion this first order macroscopic solution was multiplied by the envelope function  $f(z)$ , which described the axial distribution of hyperfine polarization in an optically thin vapor. When considering optical pumping with lamps, where the relative optical pumping rates are typically low, it is fair to approximate  $f(z)$  by Minguzzi et al., first order diffusion mode:<sup>12</sup>

$$f(z) = \sin(\pi z/L) , \quad (1)$$

where  $L$  is the length of the resonance cell. However, as discussed by Franz,<sup>13</sup> when the optical pumping rate increases this approximation is no longer valid; this point will be considered in more detail in Section III.

### III. LASER-PUMPED GAS CELL CLOCK

#### A. DIFFUSION

To determine the envelope function  $f(z)$  for the potentially high optical pumping rates associated with the use of a diode laser, we consider the thin vapor optical pumping rate equation for a two-level atom subject to diffusion in only one dimension:

$$\frac{dP}{dt} = D \frac{d^2 P}{dz^2} - \left\{ \gamma_1 + \frac{R_1}{2} \right\} P + \frac{R}{2} \quad (2)$$

where  $P$  is defined as the normalized population difference between the two levels (i.e.,  $P = (n_1 - n_2)/(n_1 + n_2)$ , where  $n_i$  is the number density of atoms in the level  $i$ ); and  $\gamma_1$ ,  $R$  and  $D$  are, respectively, the longitudinal collisional relaxation rate, the photon absorption rate (only one of the two levels is assumed to interact with the light), and the diffusion coefficient. In steady-state the solution of Eq. (2) is

$$P(z) = \left\{ \frac{R}{R + 2\gamma_1} \right\} [1 - \exp(-\alpha z)] \left\{ 1 - \exp \left\{ -\frac{\alpha(L-z)}{2} \right\} \left[ \frac{\cosh(\alpha z/2)}{\cosh(\alpha L/2)} \right] \right\} \quad (3)$$

where

$$\alpha \equiv \sqrt{\left\{ \gamma_1 + \frac{R_1}{2} \right\} / D} \quad (4)$$

Normalizing  $P(z)$  to its peak value we obtain the form of  $f(z)$  for arbitrary optical pumping rates:

$$f(z) = \frac{[1 - \exp(-\alpha z)] [\exp(\alpha L) - \exp(\alpha z)]}{[1 - \exp(-\alpha L/2)] [\exp(\alpha L) - \exp(\alpha L/2)]} \quad (5)$$

This envelope function is shown in Fig. 1 for several values of the relative photon absorption rate for the case of negligible collisional relaxation (i.e.,  $\gamma_1 = 0$ ). It should be noted that as the photon absorption rate increases, the envelope function becomes nearly constant. Thus, the

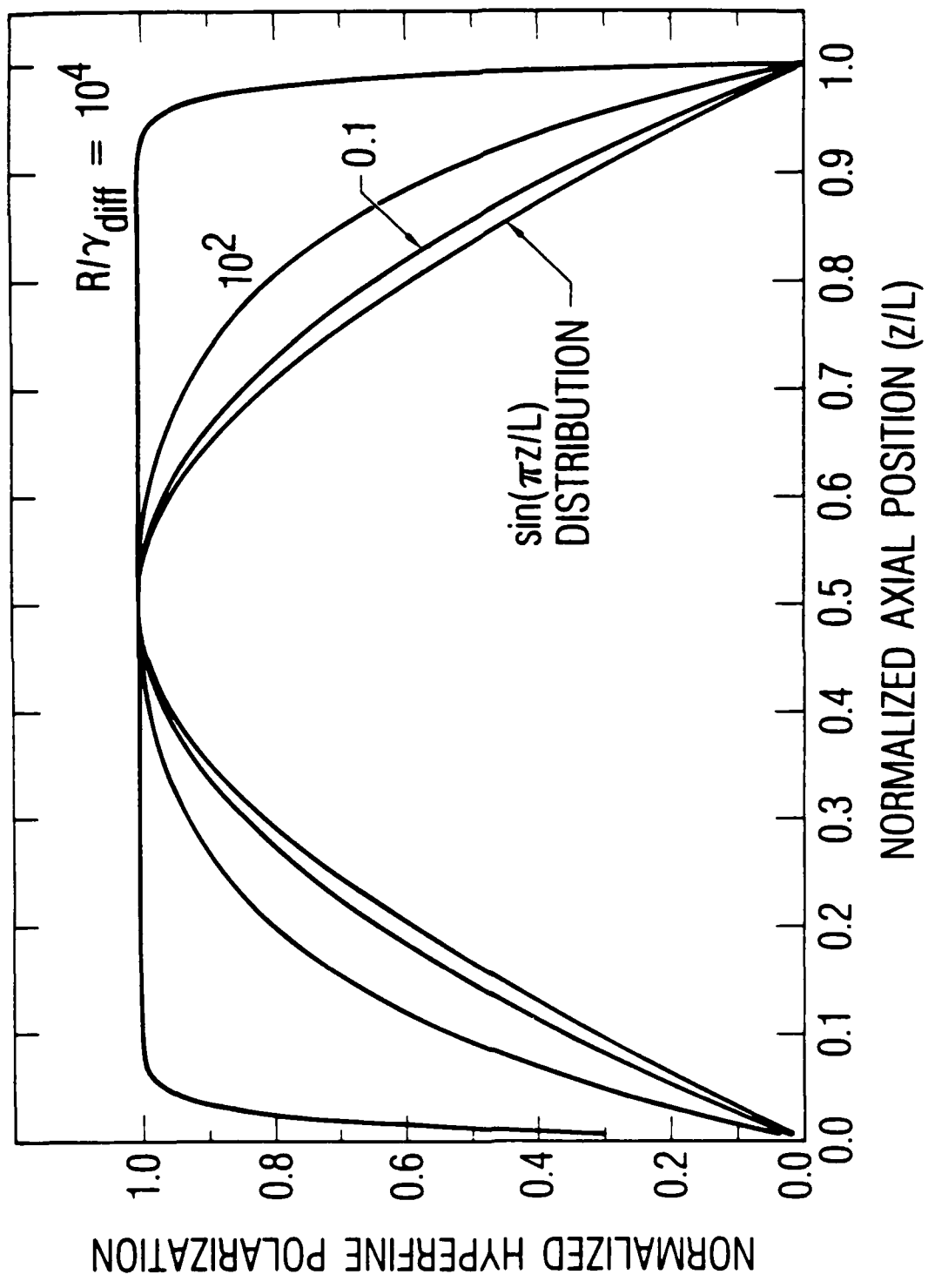


Fig. 1. Spatial Distribution of Hyperfine Polarization.

contribution of atoms closer to the resonance cell walls becomes progressively more important, implying that at high photon absorption rates the vapor is more efficiently exploited. Note also that even at relatively low photon absorption rates the vapor is more effectively exploited than the first order diffusion mode approximation would lead one to expect. This phenomenon is shown more clearly in Fig. 2, where the full width at half maximum of the envelope function is plotted as a function of the relative photon absorption rate. From this figure it is clear that once the photon absorption rate is roughly an order of magnitude greater than the rate of diffusion to the resonance cell walls (i.e.,  $D/L^2$ ), the first order diffusion mode approximation to  $f(z)$  is no longer valid.

## B. LASER STABILITY

In any attempt to realistically model the performance of a laser-pumped gas cell atomic frequency standard the frequency and intensity stability of the laser must be considered, since this is directly transferred to the frequency standard's stability via the light shift effect.<sup>14</sup> To estimate the significance of laser stability on the standard's performance, we assume that the laser intensity and frequency noise are uncorrelated, so that

$$\delta f = \frac{\partial f}{\partial \nu} \delta \nu + \frac{\partial f}{\partial I} \delta I \quad (6)$$

where  $f$ ,  $\nu$  and  $I$  correspond, respectively, to the microwave hyperfine transition frequency, the optical laser frequency, and the laser intensity. Furthermore, we imagine that in any practical device the laser frequency will be actively stabilized to the center of the atomic absorption line, so that we take  $\partial f / \partial I = 0$ . Thus, the frequency fluctuations of the atomic standard only depend on the sensitivity of the hyperfine transition frequency to the laser frequency fluctuations,  $\partial f / \partial \nu$ , and the magnitude of the laser's frequency fluctuations,  $\delta \nu$ . Obviously, it is important to minimize both of these quantities for the best performance.

As discussed by Mathur et al.<sup>14</sup> one can minimize  $\partial f / \partial \nu$  by increasing the buffer gas pressure in the resonance cell. However, one cannot increase the

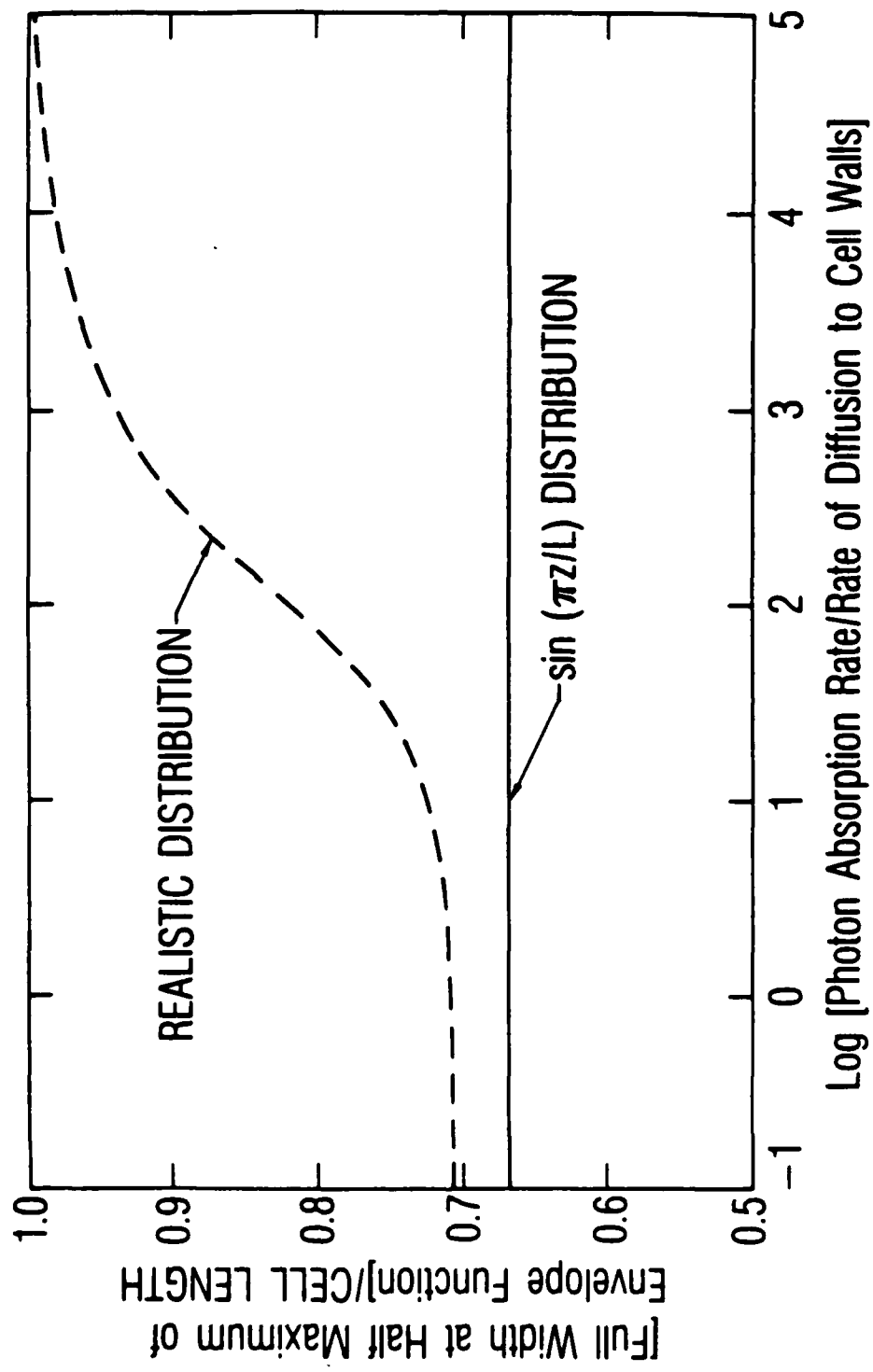


Fig. 2. Full Width at Half Maximum of the Envelope Function Normalized to the Resonance Cell Length as a Function of the Relative Photon Absorption Rate.



buffer gas pressure without bound, because once the pressure broadening of the optical absorption line exceeds the ground state hyperfine splitting, depopulation pumping cannot create a population imbalance between the two ground state hyperfine multiplets. Since pressure broadening rates are typically on the order of 10 MHz/Torr,<sup>15</sup> and since the Rb<sup>87</sup> ground state hyperfine splitting is ~7 GHz, we estimated that roughly 100 Torr of buffer gas (our calculation assumes nitrogen) was the limit on the maximum buffer gas pressure.

Recently, Ohtsu et al.<sup>16</sup> estimated the ultimate frequency stability of presently available diode lasers due to quantum noise. Basically, the ultimate frequency stability of a diode laser is related to quantum noise via three different mechanisms. Fundamentally, there is the direct quantum noise due to the phase noise associated with spontaneous emission. Additionally, however, because the index of refraction of the diode laser depends on the carrier density, the relaxation oscillations of the carrier density following a spontaneous emission event alter the phase of the entire laser field.<sup>17</sup> Furthermore, since the carrier density relates to ohmic heating, and since the index of refraction of the semiconductor material also depends on temperature, there is an additional fluctuation in the phase of the laser field following a spontaneous emission event. Together, these processes yield a white noise Allan variance for the laser frequency stability in CSP diode lasers  $\sigma_y^L(\tau)$  of  $9.02 \times 10^{-12}/\sqrt{\tau}$ .

This stability could, however, be improved by increasing the diode laser cavity's Q. An enhanced cavity Q laser could be made either by increasing the diode laser's facet reflectivity or by increasing the laser's length. In this case one would ultimately be limited by the ability to lock the diode laser frequency to an atomic absorption line. According to Shimoda,<sup>18</sup> for a perfect photodetector and 3 mW of diode laser power this limit is  $\sigma_y^L(\tau) = 8.14 \times 10^{-15}/\sqrt{\tau}$  for a linear absorption technique.

As previously mentioned it is our intent to calculate the frequency stability of the atomic standard for various diode laser intensities. However, the partial derivative  $\partial f/\partial \nu$  in Eq. (6) is evaluated at a fixed laser

intensity. Fortunately, since  $\partial f/\partial u$  is a linear function of the laser intensity, we have

$$\frac{\partial f}{\partial u} = \left( \frac{\partial^2 f}{\partial u \partial I} \right) I \quad (7)$$

and

$$\frac{\delta f}{f_0} = \left( \frac{u_0}{f_0} \right) \left( \frac{\partial^2 f}{\partial u \partial I} \right) \left( \frac{\delta u}{u_0} \right) I \quad (8)$$

where  $f_0$  and  $u_0$  are the 0-0 hyperfine transition frequency and the  $D_2$  optical transition frequency, respectively. In terms of the Allan variance Eq. (8) becomes

$$\sigma_y^c(\tau) = \left( \frac{u_0}{f_0} \right) \left( \frac{\partial^2 f}{\partial u \partial I} \right) I \cdot \sigma_y^L(\tau), \quad (9)$$

where  $\sigma_y^c(\tau)$  is the Allan variance of the clock's fractional frequency fluctuations due to laser frequency fluctuations. For 100 Torr of nitrogen, using the theory of Mathur et al.,<sup>14</sup> we calculate that  $(u_0/f_0) (\partial^2 f/\partial u \partial I) = 0.68 \text{ cm}^2/\text{mW}$ .

### C. ATOMIC STANDARD STABILITY

From the preceding discussion it is apparent that in the present work we consider the atomic standard's frequency stability to result from two uncorrelated processes. The first is the shot noise at the atomic standard's photodetector; this is equivalent to the noise process that currently limits the short-term frequency stability of gas cell atomic frequency standards. Additionally, there is the laser frequency noise which is transferred to the atomic standard via the light shift effect. If we write the clock's total white noise Allan variance as  $\sigma_y(\tau) = \Lambda/\sqrt{\tau}$ , then from Eq. (9) we have for  $\Lambda$ :

$$\Lambda^2 = a^2(I) + 0.46 \beta^2 I^2 \quad (10)$$

where  $\sigma_y^L(\tau) = \beta/\sqrt{\tau}$

$$\beta = \begin{array}{l} 9.02 \times 10^{-12} \text{ for current CSP diode lasers} \\ 8.14 \times 10^{-15} \text{ for an enhanced cavity Q diode laser} \end{array}$$

and where  $a(I)$  is the atomic standard's shot noise limit coefficient for a laser intensity  $I$  computed by our nonempirical model of the gas cell atomic frequency standard as modified by the more realistic envelope function of Eq. (5). Parameters used in the present calculation are collected in Table 1.

Table 1. Parameters Used in the Calculation of the Clock Signal Shot Noise Contribution to the Diode Laser-Pumped Gas Cell Clock's White Noise Allan Variance.

Parameter	Value
Laser Linewidth	50 MHz
Nitrogen Pressure	100 Torr
Photodetector Responsivity	0.5 amps/watt
Microwave Cavity	TE <sub>111</sub>
Microwave Cavity Length	3.8 cm
Microwave Cavity Radius	1.35 cm

#### IV. RESULTS

Figure 3 shows how the resonance cell temperatures and peak microwave Rabi frequencies that minimize the clock signal's shot noise Allan variance vary with diode laser intensity. Since the primary effect of a temperature increase in the model is to increase the rubidium number density, it is apparent from the figure that increasing laser intensities require increasing alkali vapor densities. To understand why this trend is physically reasonable, it is only necessary to realize that the signal-to-noise ratio of the clock goes roughly as  $\Delta I/\sqrt{I_e}$ , where  $\Delta I$  is the change in transmitted laser intensity due to the microwaves, and  $I_e$  is the laser intensity at the exit face of the resonance cell. If the incident laser intensity increases, then an increase in the alkali density can both increase  $\Delta I$  and decrease  $I_e$ ; thus, there is a net increase in the signal-to-noise ratio. However, for  $\Delta I$  to increase with increasing laser intensity and alkali number density (note that an increased alkali number density implies an increased spin exchange relaxation rate) there must be a concomitant increase in the peak microwave Rabi frequency. This can be understood by noting that the value of  $\Delta I$  begins to saturate when microwave power broadening of the transition lineshape first sets in.

Shown in Fig. 4a is the minimum Allan variance that can be obtained in the standard clock configuration at a particular incident laser intensity, and Fig. 4b is a magnification of the region between 0.01 and 1 mW/cm<sup>2</sup>. The three curves are for the cases where: (1) laser quantum noise, laser locking noise, and clock signal shot noise all contribute to the frequency standard's stability (i.e., we assume a commercially available diode laser); (2) only laser locking noise and clock signal shot noise contribute to the frequency standard's stability (i.e., we assume an enhanced cavity Q diode laser); and (3) only clock signal shot noise influences the standard's stability. The minimum attainable Allan variances of the diode laser-pumped rubidium gas cell atomic frequency standard for the three different cases are collected in Table 2, as well as the corresponding resonance cell temperatures and peak microwave Rabi frequencies. The most important points to note from this figure are:

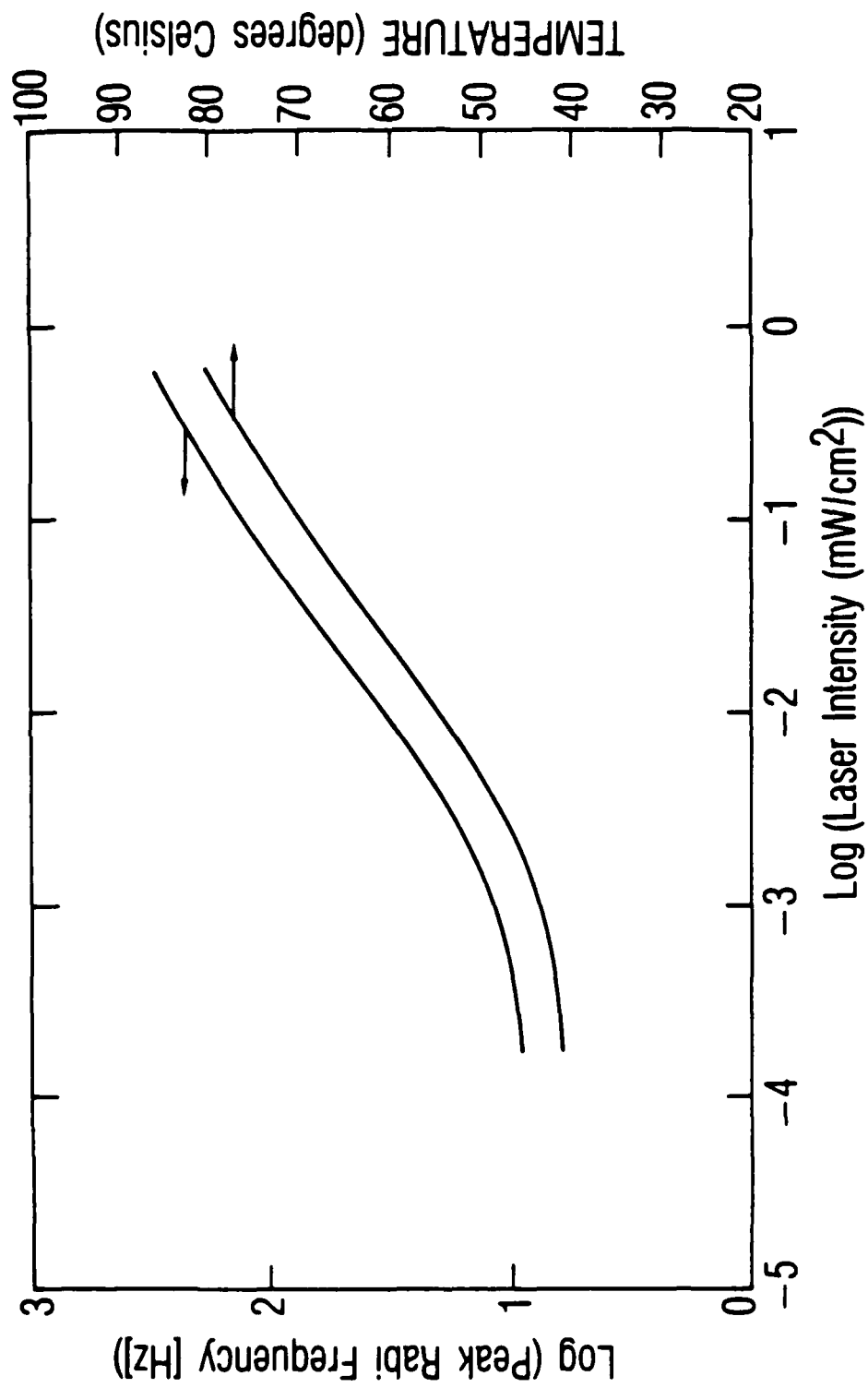


Fig. 3. Best Temperature and Rabi Frequency vs. Laser Power.

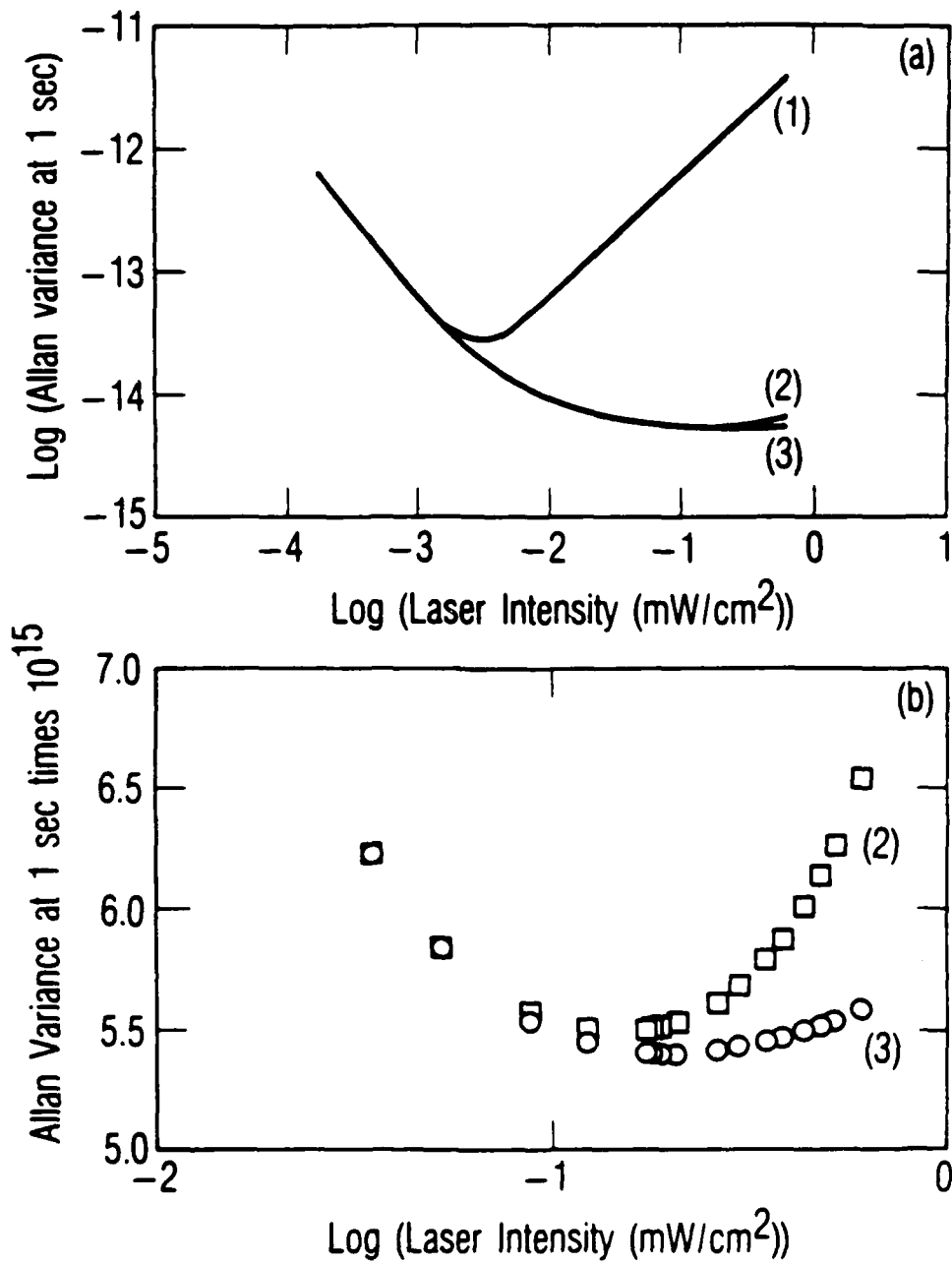


Fig. 4. Allan Variance vs. Single-Mode Laser Intensity. (a) Minimum Allan variance that can be obtained in the standard clock configuration at a particular incident laser intensity and (b) magnification of the region between 0.01 and 1 mW/cm<sup>2</sup>.

Table 2. Minimum Attainable Allan Variances of the Diode Laser-Pumped Rubidium Gas Cell Atomic Frequency Standard.

Case No.	Laser Intensity ( $\mu\text{W}/\text{cm}^2$ )	Cell Temperature ( $^{\circ}\text{C}$ )	Rabi Frequency (Hz)	Best $\sigma_y(\tau)$
1	2.6	47	17	$2.7 \times 10^{-14} / \sqrt{\tau}$
2	120	71	140	$5.5 \times 10^{-15} / \sqrt{\tau}$
3	190	74	170	$5.4 \times 10^{-15} / \sqrt{\tau}$



1. The best shot noise limited performance is obtained at relatively low incident laser intensities. Thus, there is no obvious advantage to operating a rubidium gas cell clock with a high power single-mode dye laser.
2. Whereas in presently available rubidium gas cell frequency standards the white noise Allan variance is limited by the clock signal's shot noise, the present calculations indicate that diode laser-pumped rubidium gas cell frequency standards will ultimately be limited by the frequency stability of the laser; this noise is transferred to the atomic standard via the light shift effect.

## V. SUMMARY

In the present study we have found that a diode laser-pumped gas cell atomic frequency standard has the potential for orders of magnitude improvement over existing gas cell standards, if the diode laser frequency is well stabilized. In order to put these results in the proper perspective, Fig. 5 compares the best projected Allan variances for the diode laser-pumped gas cell atomic frequency standard discussed in this report with the proposed performance of the stored  $^{201}\text{Hg}$  ion frequency standard.<sup>19</sup> Additionally, for reference, the present performance of rubidium gas cell atomic frequency standards is shown.<sup>20</sup> Though any projection of frequency stability must be taken with a grain of skepticism, it is clear that there are many avenues for order of magnitude improvement in frequency standards, and that the diode laser-pumped rubidium gas cell atomic frequency standard is a very attractive prospect.

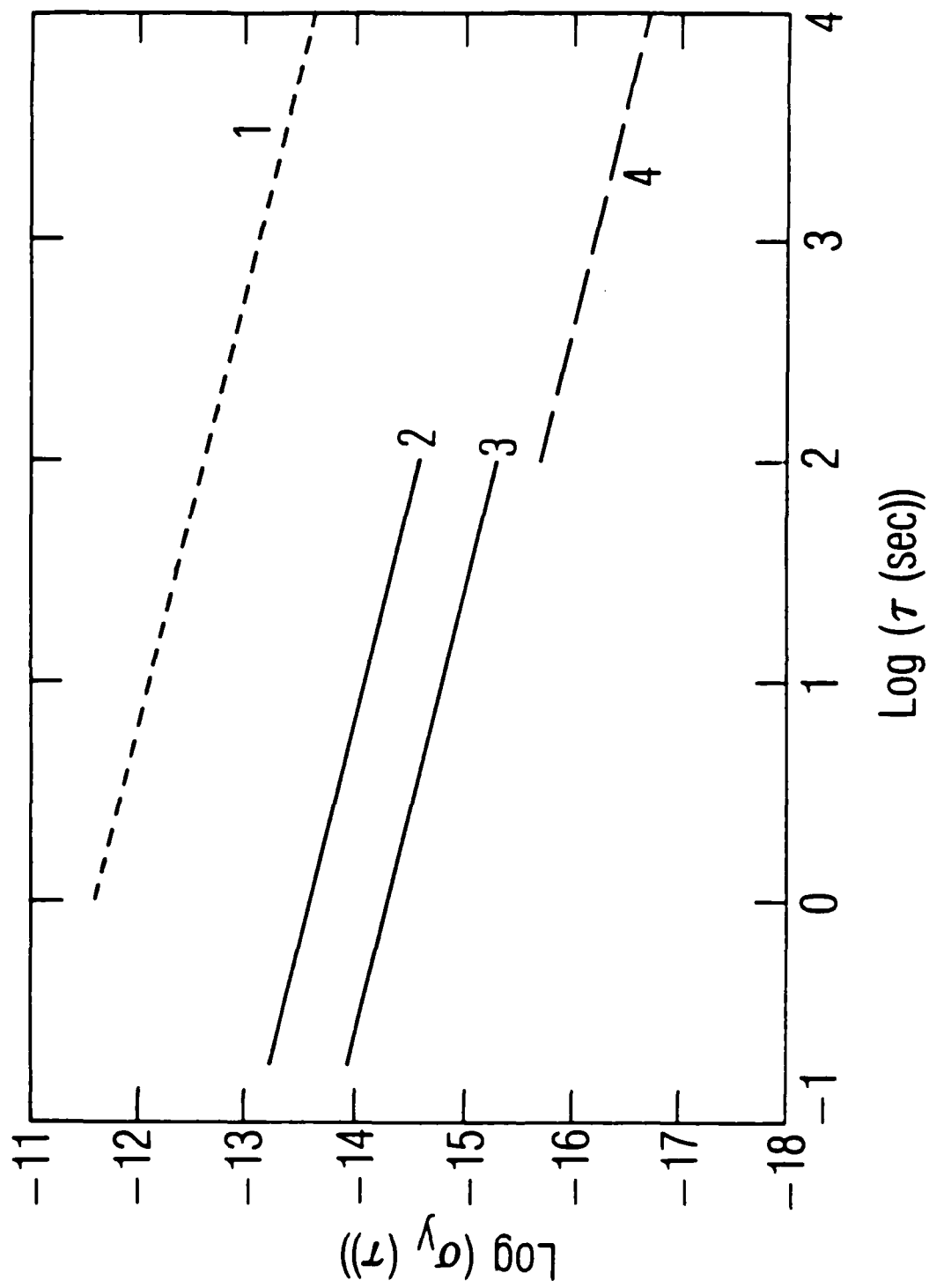


Fig. 5. Comparison of Some Proposed Atomic Frequency Standards.

## REFERENCES

1. See for example: P. Cerez, G. Avila, E. de Clercq, M. de Labachellerie, and M. Tetu in Proceedings of the 38th Annual Frequency Control Symposium (IEEE, New York, 1984), pp. 452-457.
2. L. L. Lewis, M. Feldman, and J. C. Berquist, *J. Phys. (Paris)* 42, Colloque C8, Supplement au n° 12, C8-271 (1981).
3. E. de Clercq, M. de Labachellerie, G. Avila, P. Cerez and M. Tetu, *J. Phys. (Paris)* 45, 239 (1984).
4. M. Arditì, *Metrologia* 18, 59 (1982).
5. L. Lewis and M. Feldman, in Proceedings of the 35th Annual Frequency Control Symposium (Electronic Industries Association, Washington D.C., 1981), pp. 612-624; C. H. Volk, J. C. Camparo and R. P. Frueholz, in Proceedings of the 13th Annual Precise Time and Time Interval (PTTI) Application and Planning Meeting, NASA Conference Publication 2220 (NASA, Greenbelt, MD, 1981) pp. 631-640.
6. J. Vanier, R. Kunski, A. Brisson, and P. Paulin, *J. Phys. (Paris)* 42, Colloque C8, supplement au n° 12, C8-139 (1981).
7. S. Pancharatnam, *J. Opt. Soc. Am.* 56 1636 (1966); S. Pancharatnam, *Proc. R. Soc. Lond. A.* 330, 281 (1972).
8. J. C. Camparo and R. P. Frueholz, to be published *J. Appl. Phys.*
9. J. C. Camparo and R. P. Frueholz, *Phys. Rev. A* 31, 1440 (1985).
10. J. C. Camparo and R. P. Frueholz, *Phys. Rev. A* 32, 1888 (1985).
11. R. P. Frueholz and J. C. Camparo, *J. Appl. Phys.* 57, 704 (1985).
12. P. Minguzzi, F. Strumia, and P. Violino, *Nuovo Cimento* 46B, 145 (1966).
13. F. A. Franz, *Phys. Rev. A* 6, 1921 (1972).
14. B. S. Mathur, H. Tang, and W. Happer, *Phys. Rev.* 171, 11 (1968).
15. S. Ch'en and M. Takeo, *Rev. Mod. Phys.* 29, 20 (1957).
16. M. Ohtsu, H. Fukada, T. Tako, and H. Tsuchida, *Jap J. Appl. Phys.* 22, 1157 (1983).
17. C. H. Henry, *IEEE J. Quantum Electron.* QE-18, 259 (1982).

18. K. Shimoda, *Jap. J. Appl. Phys.* 12, 1222 (1973).
19. D. J. Wineland, W. M. Itano, J. C. Bergquist and F. L. Walls, in Proceedings of the 35th Annual Frequency Control Symposium (Electronic Industries Association, Washington D.C., 1981) pp. 602-611.
20. T. J. Lynch and W. J. Riley, in Proceedings of the 15th Annual Precise Time and Time Interval (PTTI) Applications and Planning Meeting (National Technical Information Service, ADA-149-163), Springfield, VA, 1984 pp. 269-279.

## LABORATORY OPERATIONS

The Aerospace Corporation functions as an "architect-engineer" for national security projects, specializing in advanced military space systems. Providing research support, the corporation's Laboratory Operations conducts experimental and theoretical investigations that focus on the application of scientific and technical advances to such systems. Vital to the success of these investigations is the technical staff's wide-ranging expertise and its ability to stay current with new developments. This expertise is enhanced by a research program aimed at dealing with the many problems associated with rapidly evolving space systems. Contributing their capabilities to the research effort are these individual laboratories:

Aerophysics Laboratory: Launch vehicle and reentry fluid mechanics, heat transfer and flight dynamics; chemical and electric propulsion, propellant chemistry, chemical dynamics, environmental chemistry, trace detection; spacecraft structural mechanics, contamination, thermal and structural control; high temperature thermomechanics, gas kinetics and radiation; cw and pulsed chemical and excimer laser development including chemical kinetics, spectroscopy, optical resonators, beam control, atmospheric propagation, laser effects and countermeasures.

Chemistry and Physics Laboratory: Atmospheric chemical reactions, atmospheric optics, light scattering, state-specific chemical reactions and radiative signatures of missile plumes, sensor out-of-field-of-view rejection, applied laser spectroscopy, laser chemistry, laser optoelectronics, solar cell physics, battery electrochemistry, space vacuum and radiation effects on materials, lubrication and surface phenomena, thermionic emission, photo-sensitive materials and detectors, atomic frequency standards, and environmental chemistry.

Computer Science Laboratory: Program verification, program translation, performance-sensitive system design, distributed architectures for spaceborne computers, fault-tolerant computer systems, artificial intelligence, microelectronics applications, communication protocols, and computer security.

Electronics Research Laboratory: Microelectronics, solid-state device physics, compound semiconductors, radiation hardening; electro-optics, quantum electronics, solid-state lasers, optical propagation and communications; microwave semiconductor devices, microwave/millimeter wave measurements, diagnostics and radiometry, microwave/millimeter wave thermionic devices; atomic time and frequency standards; antennas, rf systems, electromagnetic propagation phenomena, space communication systems.

Materials Sciences Laboratory: Development of new materials: metals, alloys, ceramics, polymers and their composites, and new forms of carbon; non-destructive evaluation, component failure analysis and reliability; fracture mechanics and stress corrosion; analysis and evaluation of materials at cryogenic and elevated temperatures as well as in space and enemy-induced environments.

Space Sciences Laboratory: Magnetospheric, auroral and cosmic ray physics, wave-particle interactions, magnetospheric plasma waves; atmospheric and ionospheric physics, density and composition of the upper atmosphere, remote sensing using atmospheric radiation; solar physics, infrared astronomy, infrared signature analysis; effects of solar activity, magnetic storms and nuclear explosions on the earth's atmosphere, ionosphere and magnetosphere; effects of electromagnetic and particulate radiations on space systems; space instrumentation.

END

2-87-

DITIC